PART THREE
Gravitational wave emission, observations, and the link to astrophysics

https://doi.org/10.1017/S1743921315008042 Published online by Cambridge University Press

Star clusters and black holes in galaxies across cosmic time
Proceedings IAU Symposium No. 312, 2014
Y. Meiron, S. Li, F.-K. Liu & R. Spurzem, eds.

doi:10.1017/S1743921315008042

White dwarf binaries and the gravitational wave foreground

Matthew Benacquista

Center for Gravitational Wave Astronomy, University of Texas at Brownsville,
One West University Blvd, Brownsville, TX 78520, USA
email: `matthew.benacquista@utb.edu`

Abstract. Galactic white dwarf binaries will be an abundant source of gravitational waves in the mHz frequency band of space-based detectors such as eLISA. A few thousand to a few tens of thousands of these systems will be individually resolvable by eLISA, depending on the final detector configuration. The remaining tens of millions of close white dwarf binaries will create an unresolvable anisotropic foreground of gravitational waves that will be comparable to the instrument noise of eLISA at frequencies below about a mHz. Both the resolvable binaries and the foreground can be used to better understand this population. Careful choice of the initial orientation of eLISA can mitigate this foreground in searches for other sources.

Keywords. Gravitational Radiation, Ultracompact Binaries

---

1. Introduction

Ultracompact binaries with orbital periods less than a day will be the dominant source of continuous gravitational radiation in the millihertz band of the spectrum. Most of the proposed designs for space-based gravitational wave observatories are sensitive in this frequency band and the Galactic population of ultracompact binaries will produce a confusion-limited foreground at or above the designed instrumental noise. This acts as a source of noise for observations of extragalactic and cosmological gravitational wave sources, such as supermassive binary black hole inspirals, extreme mass ratio inspirals, or cosmological strings. However, the Galactic signal also contains a wealth of information about close binary evolution, the star formation history of the Galaxy, and the production of binaries through dynamical interactions in dense stellar systems. In this review, we will provide a brief introduction to the physics of gravitational radiation, a review of the current designs for eLISA, a history of population synthesis of close white dwarf binaries in the Galaxy, and conclude with a discussion of the potential of eLISA to observe this population.

2. Gravitational radiation from binary systems

Gravitational radiation is a propagating perturbation in the curvature of spacetime, which manifests itself as a time-varying perturbation of the metric. The most common coordinate (or gauge) choice used to describe a gravitational wave is the transverse-traceless gauge, which highlights the fact that gravitational radiation is a transverse wave. In the far zone, where we expect to measure the gravitational wave, we can approximate the background metric as a flat spacetime metric ($\eta_{\mu\nu}$) and the gravitational wave as a perturbation ($h_{\mu\nu}$), so:

$$g_{\mu\nu} = \eta_{\mu\nu} + h_{\mu\nu}. \tag{2.1}$$

A passing gravitational wave is measured as a strain, h. Gravitational waves generated by binary systems produce a strain in a detector whose amplitude is proportional to the orbital frequency, f, the distance to the binary, d, and the masses of the components, M_1 and M_2:

$$h \propto \frac{M_1 M_2}{(M_1 + M_2)^{1/3}} \frac{f^{2/3}}{d}. \tag{2.2}$$

The combination of masses is referred to as the "chirp mass" with:

$$\mathcal{M}_c = \left(\frac{M_1 M_2}{(M_1 + M_2)^{1/3}} \right)^{3/5} = \mu^{3/5} M^{2/5}, \tag{2.3}$$

where μ is the reduced mass and M the total mass.

For circularized binaries, the gravitational wave signal is a nearly monochromatic wave with a frequency that is twice the orbital frequency. As the binary loses energy through gravitational wave emission, the orbital frequency increases as the components slowly spiral together. The rate of change of the frequency is known as the chirp and is related to the chirp mass by:

$$\frac{df}{dt} \propto \mathcal{M}_c^{5/3} f^{11/3}. \tag{2.4}$$

Since the chirp is a measure of the rate at which gravitational wave energy is emitted by the binary, it can be considered as providing the absolute magnitude of the binary in gravitational radiation. The observed strain amplitude provides the apparent magnitude of the binary. Both depend upon the masses by the chirp mass, so the distance can be determined for a chirping binary if f, $\dot{f}$, and h are measured:

$$d = \frac{5c\dot{f}}{384\pi^2 h f^3}. \tag{2.5}$$

3. Space-based detectors

Designs for space-based gravitational wave detectors have been around since the mid 1980's. The initial design was LAGOS (Faller *et al.* 1989). This had four spacecraft flying in formation, creating an interferometer with very large arms. This design evolved to become LISA in the mid-1990s as an ESA cornerstone mission (Folkner, Bender, & Stebbins 1998). In the early 2000s, LISA was a proposed joint NASA/ESA mission with well defined characteristics (Bender 1998). In 2011, NASA withdrew from the partnership. Over the past few years, the original LISA mission has evolved into an ESA led mission, known as eLISA (Amaro Seoane *et al.* 2013). It is currently selected as the 3rd Large mission (L3) with an expected launch of 2034. Much of the design of eLISA retains features of the original LISA. The detector itself is a constellation of three spacecraft in orbit about the sun. The constellation forms a nearly equilateral triangle that tumbles and precesses as the spacecraft follow their orbits, as shown in Figure 1. Each spacecraft is maintained in a geodesic orbit by tracking an internal proof mass that is shielded from external forces. The separation between pairs of spacecraft are measured through laser links. The measurement of a passing gravitational wave appears as a strain, $h = \Delta L/L$, where the armlength, L, is the separation between spacecraft. The major sources of noise are spurious forces, position sensing, and shot noise. The spurious forces produce an acceleration noise that generates a variation in ΔL which is proportional to f^{-2}. It

https://doi.org/10.1017/S1743921315008042 Published online by Cambridge University Press

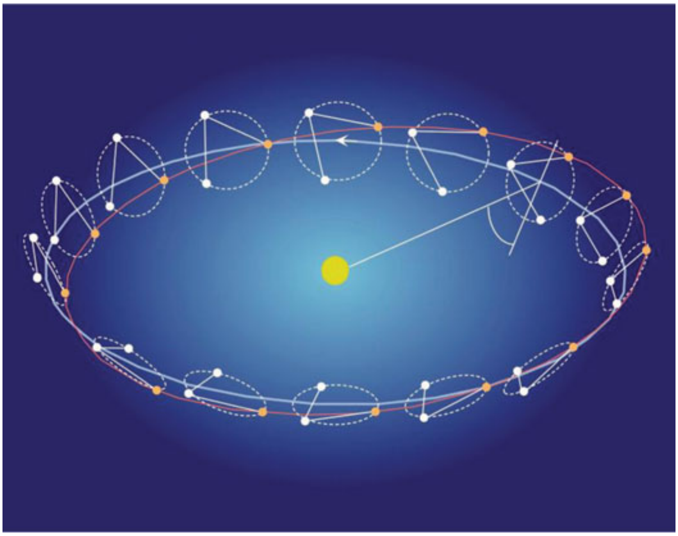

Figure 1. Orbit of the eLISA constellation about the sun.

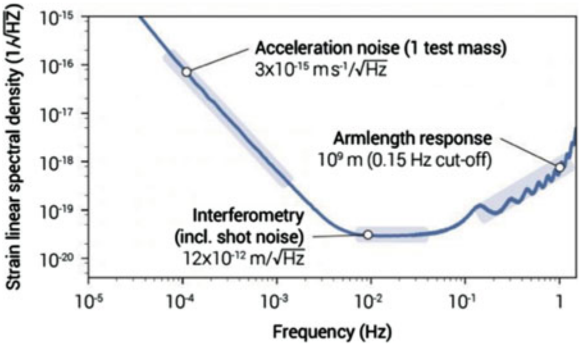

Figure 2. Typical eLISA sensitivity curve showing the contributions from acceleration, position and shot noise, and the armlength response.

dominates the instrument noise at low frequencies. Both the position and shot noise are assumed to be flat in frequency and form the floor of the detector sensitivity.

Current design choices for eLISA involve choosing armlengths that are shorter than the 5 million km of the initial LISA design. The effect of shortening the arms is to increase the acceleration and position noises inversely proportional to the change in armlength. Shortening the armlength also has the effect of decreasing the shot noise by increasing the received laser power at each spacecraft. If the shot noise drops significantly below the position noise, then additional savings can be found by lowering the laser power or decreasing the size of the optics.

Armlength also has an effect on the response of the detector for gravitational waves with wavelengths that are comparable to or shorter than the length of each arm. In this case, the effective armlength is proportional to the wavelength. Thus, the response of the detector decreases with increasing frequency beyond a threshold frequency set by the armlength of the detector, resulting in a rise in the sensitivity curve at high frequencies. Shortening the armlength then has the effect of increasing the upper frequency of the sensitivity band. See Figure 2, for a typical eLISA sensitivity curve.

The initial LISA design had three laser links, joining all three pairs of spacecraft in

https://doi.org/10.1017/S1743921315008042 Published online by Cambridge University Press

the constellation. This allowed for the synthesis of two linearly independent interferometers, and provided a coverage of the gravitational wave sky that was uniform in ecliptic longitude. The current eLISA designs call for only two pairs of spacecraft to be joined by laser links. As a result, there are four directions relative to the constellation to which the detector is insensitive to gravitational waves. These null directions trace out figure-eights in the sky as eLISA orbits the sun. The effect of this is to introduce four regions of reduced sensitivity in ecliptic longitude. The position of these regions in the sky depend upon the initial orientation of eLISA (Jani, Finn & Benacquista 2013). Judicious choice of the initial orientation of eLISA can then be used to suppress gravitational wave signals from certain regions in the sky while enhancing the response in other regions.

4. Population syntheses

Close white dwarf binaries (CWDBs) are compact enough to have short orbital periods, yet massive enough to have chirp masses that are large enough to produce meaningful strain amplitudes at typical Galactic distances. Thus, they are the most likely sources of gravitational radiation. Early estimates of the detectability of close white dwarf binaries were based on the rates of Type Ia supernovae, assuming a double degenerate progenitor scenario (Evans, Iben & Smarr 1987). Although highly uncertain, a Galactic foreground level was predicted. A more detailed analysis of the contribution of several types of ultracompact binaries to the Galactic gravitational wave signal was done in 1990 (Hils, Bender, & Webbink 1990). Based on binary evolution models of Webbink (1984), roughly 10^8 close white dwarf binaries were expected to contribute to a confusion-limited foreground in the mHz band of LAGOS. A comparison of the predicted space density with the number of CWDB's known at the time led the authors to reduce the number of modeled CWDBs by a somewhat arbitrary factor of 10. The resulting foreground still dominated the instrumental noise of LAGOS.

Ten years later, a more detailed population synthesis was performed by Nelemans, Yungelson & Portegies Zwart (2001) using binary evolution models of Hurley. This produced a similar level for the confusion noise, but was based on a population of $\sim 10^8$ CWDBs. Thus, although their population was 10 times larger than the reduced number of Hils, Bender, & Webbink (1990), the overall levels of the confusion noise were comparable. This is because the improved binary evolution models result in an average chirp mass of nearly half the value found by Hils, Bender, & Webbink (1990). By this time, LISA was the expected gravitational wave observatory. After another decade, a new population synthesis by Ruiter *et al.* (2010) using the `StarTrack` population synthesis code produced results similar to Nelemans *et al.* This indicates that the predicted value of the confusion-limited foreground is fairly robust, given the uncertainties in the binary evolution assumptions.

Much of the calibration of the population synthesis codes has been based on a small number of observed systems. In recent years, dedicated searches for white dwarf binaries such as the extreme low mass (ELM) survey have discovered a growing number of low mass detached and mass transferring systems (Kilic, *et al.* 2010; Brown *et al.* 2010; Kilic, *et al.* 2012). In addition, a number of AM CVn systems have been found in the Palomar Transient Factory (PTF) data and Sloan Digital Sky Survey data (Rau *et al.* 2010). The number of AM CVn systems found is lower than that predicted by population synthesis methods (Roelofs, Nelemans, & Groot 2007). There are two proposed solutions to this discrepancy (Nissanke *et al.* 2012). Once could be a broader spatial distribution of CWDBs, leading to an unchanged total number of CWDBs, but a lower local space density of the nearby and more easily observable AM CVn systems. Another could be

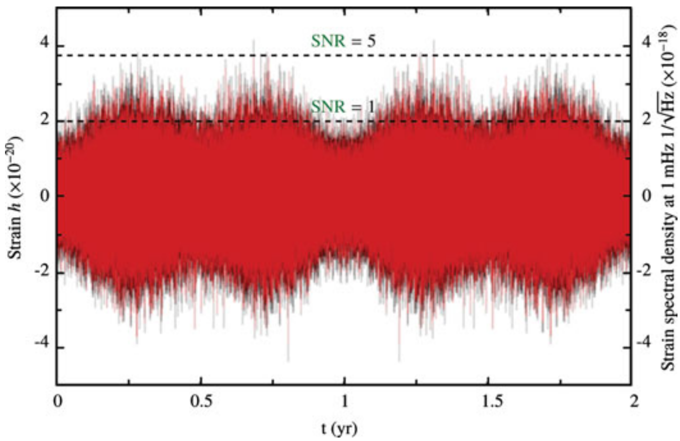

Figure 3. Level of the Galactic gravitational wave signal as a function of time. Black is the total signal, the red after removal of the resolved binaries. The yearly variation of the Galactic foreground is clearly seen. Based on the Ruiter *et al.* (2010) Galactic model.

that the conditions for stable mass transfer are more restrictive than current assumptions. This would lead to fewer AM CVns surviving after the onset of mass transfer. In this case the local space density of CWDBs would remain the same, but the number of observable AM CVns would be reduced.

5. Gravitational wave observations

The expected gravitational wave signal from the Galactic population of close white dwarf binaries can be separated into two classes—the unresolved confusion-limited foreground, and individually resolved systems. The confusion-limited foreground dominates at frequencies below a few mHz. In this region, there are multiple binaries within each resolvable frequency bin. If these overlapping signals cannot be disentangled, then they appear as a stochastic noise. The distribution of CWDBs in the sky is anisotropic with the majority of them located in the direction of the Galactic center. Consequently, the level of the foreground noise varies as the sensitivity pattern of eLISA passes over the Galactic center, as shown in Figure 3. Since the confusion foreground dominates in the frequency band where acceleration noise is the main contributor to the instrument noise, a reduction in the armlength tends to reduce the contribution of the foreground signal to the overall noise at low frequencies. See Figure 4, for an illustration of the confusion noise relative to different eLISA armlength choices.

The modulation of the confusion foreground may be used to identify and separate the foreground from the instrument noise. If the spectral slope of the signal can be determined, it may also be possible to constrain star formation histories of the Milky Way (Yu & Jeffery 2013).

The resolvable signals generally come from high-mass or high-frequency systems. These systems are very bright and can be detected from anywhere in the Galaxy. Thus, the resolvable systems will provide a complete census of double degenerate progenitors to type Ia supernovae (Stroeer, Benacquista, & Ceballos 2013). Additionally, some of the resolvable systems will have measurable chirps and so their distances can also be measured. This may provide a better understanding of the spatial distribution of the massive, high-frequency population of CWDBs in the Galaxy.

If a binary can be resolved, its sky location can be determined through modulations in

https://doi.org/10.1017/S1743921315008042 Published online by Cambridge University Press

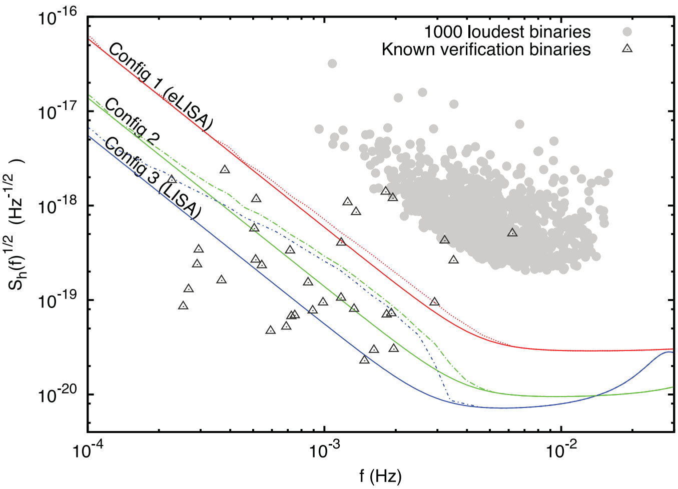

Figure 4. Sensitivity curves for 5, 2, and 1 million km armlengths. The solid lines show the sensitivity set by the measurement noise while the dashed curves include an estimate of the confusion-limited foreground. Known binaries are indicated with black triangles and resolved binaries from a population synthesis are grey circles. Figure taken from Littenberg, *et al.* (2013).

the amplitude, frequency, and polarization of the observed gravitational wave as eLISA executes its tumbling motion during its orbit about the sun. Typical angular resolutions for these systems will be below a few square degrees. This angular resolution will be sufficient to identify the compact binary population of individual globular clusters.

The gravitational wave strain amplitude produced by close white dwarf binaries is too small for any extragalactic systems to be observed. However, stellar mass binary black holes will have substantially larger chirp masses and may be detectable at the distance of the Virgo cluster galaxies. The field population of stellar mass black holes is small enough that fewer than a couple of Galactic systems may exist in the eLISA band. The increased number of galaxies gained by looking out to the Virgo cluster may bring this number up to 10 or so, if extragalactic systems are included (Benacquista *et al.* 2014).

The potential for detection of extragalactic sources within the Virgo cluster provides incentive to take advantage of the ability to suppress eLISA sensitivity to regions of the sky. The bulk of the foreground signal will come from the large population of CWDBs in the direction of the Galactic center. Choosing the initial orientation of eLISA so that one of the nulls passes over the Galactic center reduces the sensitivity of eLISA to the strongest source of the foreground. This orientation also reduces the sensitivity of eLISA to signals from the direction of the Virgo cluster, but the two sensitivity nulls that cause these reductions are out of phase with each other. Thus, the sensitivity to the Virgo cluster is at its highest during those times that the sensitivity to the Galactic center is at its lowest (Jani, Finn & Benacquista 2013).

6. Conclusions

Space-based interferometry will be the most likely detector for observations of gravitational waves in the mHz band. The most numerous sources for gravitational radiation in this band are the Galactic population of close white dwarf binaries. Decades of population synthesis work has produced a robust prediction of the nature of the gravitational wave signal from this population. There will be a confusion-limited foreground signal from millions of CWDBs at frequencies below 3 mHz. This signal will be comparable or larger than the instrument noise for several designs of eLISA. In addition to the foreground, a few thousand of Galactic CWDBs will be individually resolvable. These systems will be high mass/high frequency sources, and will be detectable from throughout the Galaxy. Because the distribution of CWDBs is concentrated toward the Galactic center, the foreground is anisotropic in the sky and it will be modulated as the eLISA sensitivity peak sweeps over the Galactic center during its orbit about the sun. Some black hole binaries produced in globular clusters may also be observable at extragalactic distances, with the majority of them coming from the Virgo cluster. By choosing the initial orientation of the eLISA constellation, it will be possible to suppress the foreground signal while enhancing the sensitivity to sources in the Virgo cluster.

References

Amaro Seoane, P., *et al.* (The eLISA Consortium) 2013, *arXiv*, 1305.5720

Benacquista, M., Hinojosa, J., Mata, A., & Belczynski, K. 2014, *arXiv* 1410.1177

Bender, P. L. 1998, *Bull. Amer. Astron. Soc.*, 30, 1326

Brown, W. R., Kilic, M., Allende Prieto, C., & Kenyon, S. J. 2011, *ApJ*, 723, 1072

Evans, C. R., Iben, I., & Smarr, L. 1987, *ApJ*, 323, 129

Faller, J. E., Bender, P. L., Hall, J. L., & Hils, D., Stebbins R. T. 1989, *Adv. Space Res.*, 9, 107

Folkner, W. M., Bender, P. L., & Stebbins, R. T. 1998, *Publication 97-16*, Jet Propulsion Laboratory, California Institute of Technology, Pasadena, CA.

Hils, D., Bender, P. L., & Webbink, R. F. 1990, *ApJ*, 360, 75

Jani, K. P., Finn, L. S., & Benacquista, M. J. 2013, *arXiv*, 1306.3253

Kilic, M., Brown, W. R., Allende Prieto, C., Kenyon, S. J., & Panei, S. J. 2010, *ApJ*, 716, 122

Kilic, M., Brown, W. R., Allende Prieto, C., Kenyon, S. J., Heinke, C. O., Agüeros, M. A., & Kleinman, S. J. 2012, *ApJ* 751, 141

Littenberg, T. B., Larson, S. L., Nelemans, G., & Cornish, N. J. 2013, *MNRAS*, 429, 2361

Nelemans, G., Yungelson, L. R., & Portegies Zwart, S. F. 2001, *A&A*, 375, 890

Nissanke, S., Vallisneri, M., Nelemans, G., & Prince, T. A. 2012, *ApJ*, 758, 131

Rau, A., Roelofs, G. H. A.., Groot, P. J., Marsh, T. R., Nelemans, G, Steeghs, D., Salvato, M., & Kasliwal, M. M. 2010, *ApJ*, 708, 456

Roelofs, G. H. A.., Nelemans, G., & Groot, P. J. 2007, *MNRAS* 382, 685

Ruiter, A. J., Belczynski, K., Benacquista, M., Larson, S., & Williams, G. 2010, *ApJ*, 717, 1006

Stroeer, A., Benacquista, M., & Ceballos, F. 2013, in *Proc. IAU Symposium 281: Binary Paths to Type Ia Supernovea Explosions*, ed. R. Di Stefano, M. Orio & M. Moe (Cambridge University Press), 217

Webbink, R. F. 1984, *ApJ*, 277, 355

Yu, S. & Jeffery, S. 2013, *MNRAS*, 429, 1602

https://doi.org/10.1017/S1743921315008042 Published online by Cambridge University Press